Research Article

Synthesis of a Mechanically Planar Chiral Rotaxane Ligand for Enantioselective Catalysis

Andrew W. Heard[1] Stephen M. Goldup[1,2]*
[1]School of Chemistry, University of Southampton, Highfield, Southampton, SO17 1BJ, UK
[2]Lead Contact
*Correspondence: s.goldup@soton.ac.uk

SUMMARY

Rotaxanes are interlocked molecules in which a molecular ring is trapped on a dumbbell-shaped axle due to its inability to escape over the bulky end groups, resulting in a so-called mechanical bond. Interlocked molecules have mainly been studied as components of molecular machines, but the crowded, flexible environment created by threading one molecule through another, reminiscent of the active site of an enzyme, has also been explored in catalysis and sensing. However, so far the applications of one of the most intriguing properties of interlocked molecules, their ability to display stereogenic units that do not rely on the stereochemistry of their covalent subunits, termed "mechanical chirality", have yet to be properly explored and prototypical demonstration of the applications of mechanically chiral rotaxanes remain scarce. Here we describe a mechanically planar chiral rotaxane-based Au complex that mediates a cyclopropanation reaction with stereoselectivities that are comparable with the best conventional covalent catalyst reported for this reaction.

Chirality, Rotaxanes, Stereoselective, Catalysis

The Bigger Picture

Molecules that exist in non-identical mirror image forms, like the relationship between left and right hands, are referred to as chiral, from the Greek for hand. Chirality can arise due to various molecular features in which atoms are held in fixed orientations that are themselves chiral and typically such "stereogenic units" are maintained by direct bonds between atoms. Molecular chirality can also arise by threading a dumbbell shaped molecule through a molecular ring to generate a structure called a rotaxane. However, these molecules have not been investigated significantly because, until recently, they were extremely hard to make in one mirror image form. Here we report the first example of a catalyst based on such a "mechanically chiral" rotaxane. Catalysis with chiral molecules is extremely important in modern chemistry as it is one of the most efficient ways to make chiral molecules for applications in healthcare and other areas. Our results demonstrate that mechanically chiral molecules are a promising and underexplored platform for generating such catalysts.

INTRODUCTION

Interlocked molecules such as rotaxanes, in which a dumbbell shaped axle is threaded through a macrocycle, and catenanes, in which two or more macrocycles are held together in a manner akin to links in a chain,[1] are most commonly investigated as components of molecular machines,[2] building on the pioneering work of Stoddart and Sauvage who were awarded the Nobel Prize for their efforts in 2016.[3,4,5] In contrast, one of the most intriguing structural properties of interlocked molecules, their ability to display enantiotopic stereogenic elements that do not rely on covalent stereochemistry,[6] has received much less attention, despite the possibility of such enantiomerism being discussed early in the development of the field.[7,8] Such "mechanical" stereogenic units can arise due to desymmetrisation of one of the covalent sub-units by the relative position of the other (co-conformational chirality), the combination of sub-units with appropriate symmetry properties (conditional mechanical chirality) or due to the unconditional topology of the mechanical bond itself (Figure 1a).[6]

Figure 1. Different forms of chirality in mechanically and covalently bonded molecules
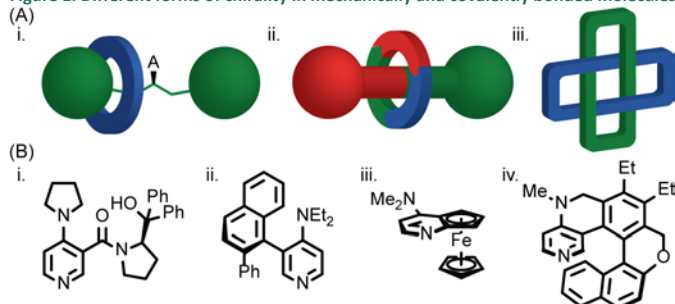
(A) Examples of i. co-conformational, ii. conditional mechanical and iii. unconditional topological stereogenic units.

(B) Examples of covalently bonded chiral acyl transfer catalysts based on i. point,[9] ii. axial,[10] iii. planar[11] and iv. helical[12] stereogenic units.

The relative paucity of even prototypical applications of mechanically chiral molecules is at least in part because enantiopure samples were historically hard to synthesise, with the pioneering work, carried out by Vögtle, Okamoto and Sauvage,[13,14] requiring the use of chiral stationary phase HPLC to separate the enantiomeric products from a racemic mixture. Using this approach, Vogtle and co-workers showed that mechanically planar chiral rotaxanes and topologically chiral catenanes displayed strong electronic circular dichroism (CD),[13] Hirose and co-workers disclosed a mechanically planar chiral rotaxane that selectively binds and senses the enantiomers of small chiral molecules,[15] and Takata and co-workers demonstrated that the mechanically planar chiral stereogenic unit can direct the helical twist of a poly-diacetylene material.[16] More recently, Saito and co-workers demonstrated the separation of co-conformationally mechanically planar chiral rotaxanes and used the link between the rate of racemisation and co-conformational motion to determine the energy barrier for shuttling,[17] and Credi and co-workers demonstrated a co-conformationally mechanically planar chiral molecule that shuttles between achiral and chiral states, the latter of which could be biased by the binding of a small chiral guest.[18]

However, of these unusual forms of stereochemistry, only co-conformational point chirality has been exploited in catalysis; in 2015 Leigh and co-workers demonstrated an enantioselective co-conformationally covalent point chiral organocatalyst (Figure 1Ai) that mediated enamine and iminium activation.[19,20,21] In contrast, the full complement of covalent stereogenic units,[22] including point,[23] axial,[24] planar[25] and helical[26] chirotopic elements,[27] have been applied in the development of new scaffolds to mediate enantioselective processes (Figure 1a) since the Nobel Prize was awarded in 2001 to Noyori, Knowles and Sharpless for their contributions to the development of enantioselective catalysis.[28, 29, 30] Indeed, recent work has aimed at expanding the mechanisms by which stereochemical information is transferred to the reaction space including the use of chiral counterions,[31] chiral-at-metal systems,[32] helical artificial[33] and natural[34] polymers, chiral solvents,[35] chiral capsules[36] and other confined environments.[37]

Building on our recent effort to improve access to mechanically chiral molecules through the use of chiral derivatising units[38,39] and auxiliaries,[40] here we demonstrate the first example of enantioselective catalysis with a mechanically planar chiral rotaxane, one of the simplest conditional mechanical stereogenic units, which arises when an achiral C_{nh} macrocycle encircles an achiral C_{nv} axle.[6] Our rotaxane catalyst, whose structure was not designed or optimised, displays enantioselectivities in an Au^I-mediated cyclopropanation reaction comparable to the best reported covalent catalyst.[41] Our results suggest that mechanical stereochemistry has untapped potential in the development of new enantioselective catalytic systems.

RESULTS AND DISCUSSION

Synthesis and Characterisation of Mechanically Planar Chiral Complex [Au(6)(Cl)]

To demonstrate the potential of mechanical stereochemistry in catalysis we selected a Au^I-mediated reaction for our study; Au^I-mediated reactions are inherently difficult to render enantioselective as a result of the linear coordination chemistry of the metal ion.[42] These challenges are typically overcome through the use of large, monodentate ligands that project

substituents into the reaction space, or the use of di-Au[I] complexes in which aurophilic interactions pre-organise the complex with one metal ion playing the role of catalyst and the other of a structural unit,[43] although employing secondary interactions in bifunctional catalysts is a promising emerging strategy.[44,45] Given that we have previously shown that the mechanical bond can be used to project steric bulk around an Au[I] centre, leading to highly diastereoselective catalysis,[46] we proposed that similar effects might be observed in the case of a mechanically chiral derivative, leading to enantioselective catalysis.

Rotaxane Au[I] complex [Au(**6**)(Cl)] was synthesised using our small macrocycle modification[47] of Leigh's active template[48] Cu-mediated alkyne-azide cycloaddition reaction (AT-CuAAC),[49] employing amino-acid derived azide **1** as a stereo-differentiating unit,[39] borane protected propargylic phosphine **2** as the alkyne coupling partner, and readily available C_{1h} (C_s) symmetric macrocycle **3**,[50] as the key mechanical bond forming step. We typically carry out the AT-CuAAC reaction in the presence of excess N^{i}Pr$_2$Et, which accelerates the reaction by favouring the formation of the key macrocycle-Cu[I]-acetylide complex intermediate. However, in this case, N^{i}Pr$_2$Et was found to cause epimerisation of the azide stereocentre, resulting in a mixture of all four possible stereoisomeric products. Replacing N^{i}Pr$_2$Et with Proton Sponge® drastically reduced the epimerisation side reaction, allowing the mixture of diastereomeric phosphine oxides **4** to be separated [51] with excellent stereochemical purity after demetallation and oxidative work-up. Using this sequence we were able to isolate rotaxanes (*S*,*R*$_{mp}$)-**4** (98% *ee*, >99 : <1 *dr*) and (*S*,*S*$_{mp}$)-**4** ((*S*,*S*$_{mp}$)-**4**-(*R*,*S*$_{mp}$)-**4**-(*S*,*R*$_{mp}$)-**4** = 98.4 : 1.0 : 0.6, *i.e.* >98% *ee* in the mechanical stereogenic unit) in an acceptable combined yield of 54%. Alkylation of diastereomer (*S*,*R*$_{mp}$)-**4** with BnI erased the covalent stereogenic unit to produce rotaxane (*R*$_{mp}$)-**5** in which the mechanical bond provides the sole stereogenic unit in excellent yield and enantiopurity (81%, 98% *ee*). Subsequent reduction of the phosphine oxide moiety and coordination of AuCl produced Au[I] precatalyst [Au((*R*$_{mp}$)-**6**)(Cl)], the enantiopurity of which was assumed to be the same as that of (*R*$_{mp}$)-**5** (98% *ee*) as the mechanical bond is configurationally stable. The same procedures starting from (*S*,*S*$_{mp}$)-**4** produced [Au((*S*$_{mp}$)-**6**)(Cl)] (98% *ee*).

Scheme 1. Synthesis of Mechanically Planar Chiral Rotaxane Pre-Catalysts
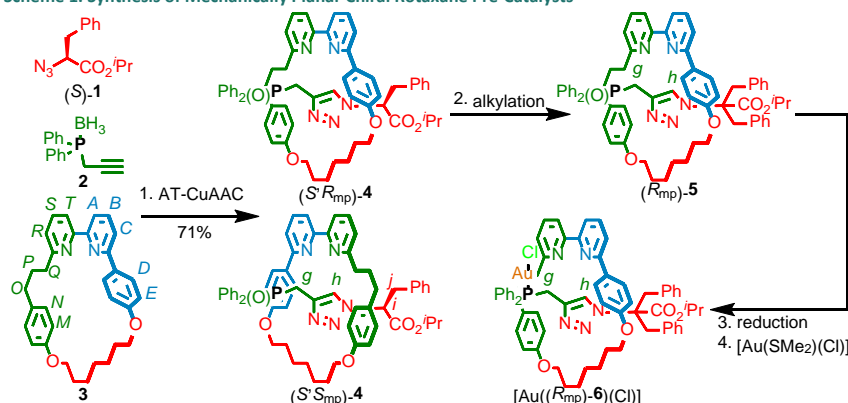
Reagents and conditions: 1. (i) [Cu(MeCN)$_4$]PF$_6$, ¹H-sponge®, CH$_2$Cl$_2$, rt, 8 h; (ii) KCN, MeOH-CH$_2$Cl$_2$ (1 : 1), rt, 30 min; (iii) H$_2$O$_2$ (35% w/w in H$_2$O), CH$_2$Cl$_2$, rt, 5 min. 72% combined yield over 3 steps prior to separation of diastereomers. (*S*,*R*$_{mp}$)-**4**: 30%, 98% *ee*, >99 : <1 *dr*; (*S*,*S*$_{mp}$)-**4**: 24%, (*S*,*S*$_{mp}$)-**4**-(*R*,*S*$_{mp}$)-**4**-(*S*,*R*$_{mp}$)-**4** = 98.4 : 1.0 : 0.6. 2. LiHMDS, THF, −78 ºC then, BnI, −78 to rt, 18 h. (*R*$_{mp}$)-**5**: 81% (98% *ee*). (*S*$_{mp}$)-**5** 63% (98% *ee*; not shown, see ESI). 3. HSiCl$_3$, NEt$_3$, PhMe, CH$_2$Cl$_2$, 100 ºC, 3 d. 4. (Me$_2$S)AuCl, CH$_2$Cl$_2$, rt, 1 h. (*R*$_{mp}$)-**5**: 64% yield over two steps (98% *ee*). (*S*$_{mp}$)-**6**: 62% (98% *ee*; not shown, see ESI).

Rotaxanes **4**, **5** and [Au(**6**)(Cl)] were isolated and characterised in full by NMR, MS, HPLC (**4** and **5**) and CD (see ESI for full details). The absolute stereochemistries of phosphine oxides (*S*,*R*$_{mp}$)-**4** and (*S*,*S*$_{mp}$)-**4**[52] were assigned by single crystal x-ray diffraction[53] (SC-XRD, Figure 2A and 2B); the internal stereochemical reference provided by the azide-derived unit allowed the orientation of the macrocycle to be determined unambiguously and the stereochemical labels were assigned using our established approach (see ESI for details).[6] The absolute stereochemistry of rotaxanes **5** and [Au(**6**)(Cl)] were inferred by noting that the mechanical stereochemistry of the corresponding diastereomeric starting materials cannot be altered in subsequent reactions.

Figure 2. Characterization of Rotaxanes 4 and 5
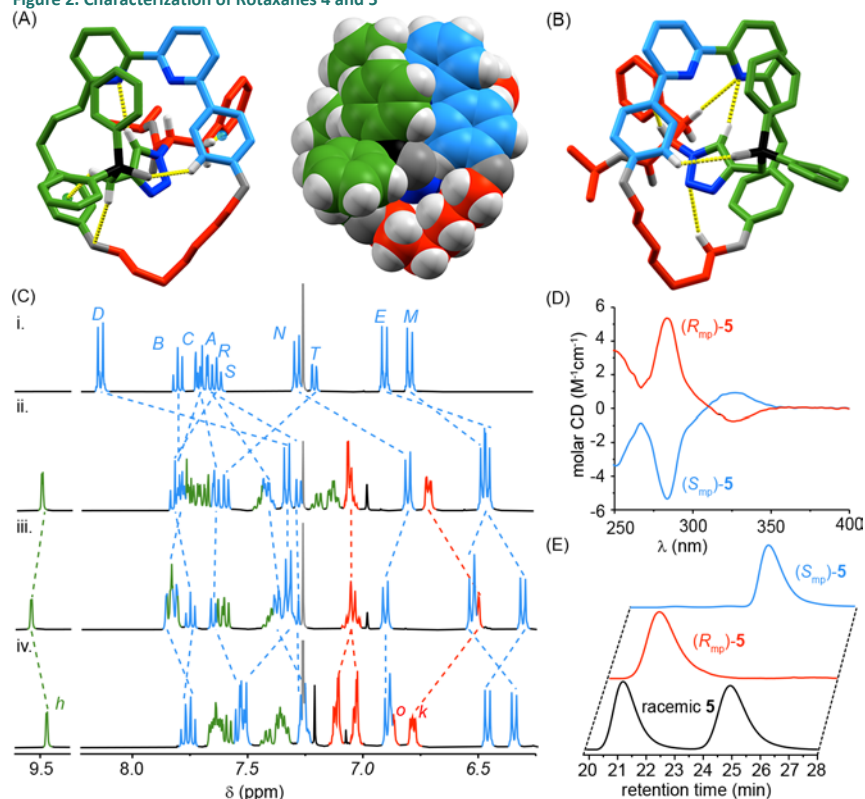
(A) Solid state structure of (S,R_{mp})-**4** with selected intercomponent interactions highlighted (atom labels and colours (O = dark grey, N = dark blue) as in Scheme 1, selected distances (Å): $H_g \bullet \bullet \bullet O$ = 2.4, $H_g \bullet \bullet \bullet$ centroid = 2.6, $H_h \bullet \bullet \bullet N$ = 2.5, $H_j \bullet \bullet \bullet$ centroid = 3.2, $H_E \bullet \bullet \bullet O$ = 2.5).

(B) Solid state structure of (S,S_{mp})-**4** with selected intercomponent interactions (atom labels and colours (O = dark grey, N = dark blue) as in Scheme 1, selected distances (Å): $H_h \bullet \bullet \bullet N$ = 2.4, $H_i \bullet \bullet \bullet C$ = 2.6, $H_j \bullet \bullet \bullet N$ = 2.7, $H_E \bullet \bullet \bullet O$ = 2.7). It should be noted that the asymmetric unit contains an oxidised derivative of (S,S_{mp})-**4** as a disordered impurity.[52] The figure depicts the component of the unit cell that is unaffected by this disorder.

(C) Partial ^1H NMR (CDCl$_3$, 400 MHz, 298 K) of i. macrocycle **3**, ii. rotaxane (S,R_{mp})-**4**, iii. rotaxane (S,S_{mp})-**4**, iv. rotaxane (R_{mp})-**5**. Selected signals are assigned and color coded (see Scheme 1 for labels; H_k and H_o, assigned arbitrarily, are the *ortho* protons of the diastereotopic axle benzyl groups). Signals corresponding to macrocycle **3** are all shown in blue for clarity.
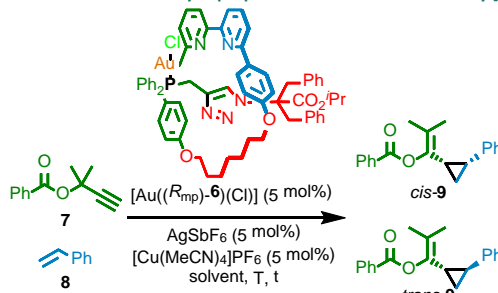
The ^1H NMR spectra of diastereomers (S,R_{mp})-**4** and (S,S_{mp})-**4** (Figure 2Cii and 2Ciii respectively) display the typical features of such interlocked molecules;[47] many of the signals corresponding to the axle and macrocycle components, including H_D, H_E, H_M, and H_N are shielded relative to the non-interlocked macrocycle (Figure 2Ci), and triazole proton H_h appears at high chemical shift due to the formation of an intercomponent C-H•••N hydrogen bond with the bipyridine, as observed in the solid state structures (Figures 2A and 2B). However, their ^1H NMR spectra are clearly distinct, in keeping with the diastereomeric relationship between the two products, as are their CD spectra (see ESI). Alkylation of rotaxanes **4** to give rotaxanes **5**, produced materials with identical ^1H NMR spectra (Figure 2Biv) but mirror image CD spectra (Figure 2D), in keeping with the enantiomeric relationship between these products. Strikingly, in addition to the expected shielding/deshielding of signals, the aromatic protons corresponding to the diastereotopic benzylic units of the axle in rotaxanes **5** are clearly distinct (e.g. benzylic *ortho* protons H_k and H_o), suggesting that the stereochemistry of the mechanical bond is well expressed onto the axle.

Enantioselective Cyclopropanation Reactions Mediated by Rotaxane [Au((R_{mp})-6)(Cl)]

With precatalyst [Au((R_{mp})-**6**)(Cl)] in hand, we investigated its behaviour in the enantioselective Au^I-mediated variant of the Ohe-Uemura[54] cyclopropanation of alkenes by propargylic esters originally reported by Toste and co-workers using (R)-DTBM-SEGPHOS®(AuCl)$_2$ and resulting in stereoselectivities from 60 to 94% *ee*.[41] More recently, Fuerstner and co-workers reported a mono-dentate binol-derived phosphoramite ligand for

the same reaction,[55] and Toste and co-workers reported a reaction system that employs Au nanoclusters embedded in a chiral self-assembled monolayer.[56]

Table 1. Optimization of an Enantioselective Cyclopropanation Reaction Mediated by [Au(6)(Cl)][a]

Entry	Solvent	T (°C)	t (h)	cis : trans[b]	er_cis[c]	er_trans[c]
1	CDCl$_3$	25	1	95 : 5	72 : 28	58 : 42
2[d]	CDCl$_3$	25	1	n.r.	-	-
3[e]	CDCl$_3$	25	1	95 : 5	29 : 71	42 : 58
4	MeNO$_2$	25	1	87 : 13	53 : 47	65 : 35
5	CD$_2$Cl$_2$	25	1	83 : 17	64 : 36	66 : 34
6	CCl$_4$	25	1	86 : 14	71 : 29	58 : 42
7	PhMe	25	1	85 : 15	69 : 31	56 : 44
8[f]	CDCl$_3$	0	6	94 : 6	79 : 21	62 : 38
9	CDCl$_3$	−35	24	96 : 4	79 : 21	61 : 39
10[g]	MeNO$_2$	25	0.5	>20 : <1	16 : 84	-

[a][Au(**6**)(Cl)] with 84% *ee* was used for screening experiments unless otherwise stated. [b]Determined by ^{1}H NMR analysis of the crude reaction product using C$_2$Cl$_4$H$_2$ as an internal standard (yield determination). [c]Determined by HPLC. [d]Reaction was conducted without the Cu[I] additive. [e]Reaction conducted with [Au((S$_{mp}$)-**6**)(Cl)]. [f]Reaction conducted with [Au(**6**)(Cl)] with *er* = 99 : 1 stereopurity. [g]Reaction outcome reported by Toste and co-workers for (R)-DTBM-SEGPHOS®(AuCl)$_2$.[41]
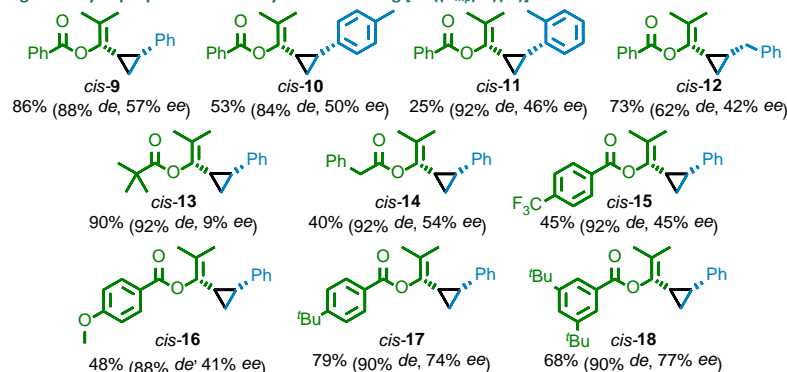
Under conditions previously optimised for an analogous achiral rotaxane-based catalyst,[46] [Au((R$_{mp}$)-**6**)(Cl)] mediated the reaction of benzoyl ester **7** with styrene (**8**) to produce cyclopropanes **9** in excellent selectivity for the *cis* diastereomer (Table 1, entry 1). The role of Cu[I] additive is to bind to the bipyridine moiety, preventing the Lewis base inhibition of the Au[I] centre; reactions in the absence of Cu[I] were unsuccessful (entry 2).[46] Other cationic additives failed to activate the catalyst (see ESI). Analysis of the purified major diastereomer by chiral stationary phase HPLC revealed reasonable enantioselectivity for (1S,2R)-**9** (*er* = 72 : 28).[57] As expected, replacing [Au((R$_{mp}$)-**6**)(Cl)] with [Au((S$_{mp}$)-**6**)(Cl)] produced **9** with opposite enantioselectivity (entry 3). Variation of the solvent led to changes in the observed *er* of *cis*-**9**, but no significant improvement (entries 4-7). Cooling the reaction to 0 °C improved the *er* of the major diastereomer to 79 : 21 (entry 8). Cooling the reaction mixture further led to no significant improvement and slowed the process considerably (entry 9). For comparison, the same reaction mediated by (R)-DTBM-SEGPHOS®(AuCl)$_2$ reported by Toste and co-workers produces cyclopropanes **9** in moderately higher and opposite stereoselectivity (entry 10).

With suitable conditions in hand (Table 1, entry 8) we performed a brief investigation of the effect of substrate on the stereoselectivity of reactions mediated by [Au((R$_{mp}$)-**6**)(Cl)] (Figure 3). Variation of the styrene component in the reaction of benzoate ester **7** gave cyclopropanes **10** and **11** in similar *ee* and *de* to **9**, although the yield of the reaction was much lower in the case of 2-Me substituted product **11**. Replacing styrene with allyl benzene gave cyclopropane **12** in reasonable enantioselectivity but lower diastereoselectivity, as has previously been observed for aliphatic alkenes.[41] Conversely, variation of the propargylic ester component had a significant effect on the reaction stereoselectivity. Whereas (R)-DTBM-SEGPHOS®(AuCl)$_2$ is reported to deliver higher stereoselectivity with the pivaloyl derivative of propargyl ester **7**,

in the case of [Au((R_{mp})-**6**)(Cl)], cyclopropane **13** was produced with almost no enantioselectivity. Pleasingly, phenylacetate ester-derived cyclopropane **14** was produced in comparable selectivity to **9**, confirming that α-alkyl esters are tolerated by [Au(**6**)(Cl)] and suggesting that the steric bulk of the pivolyl moiety is responsible for the loss of stereoselectivity in the case of **13**. Variation of the benzoyl moiety to introduce strongly electron withdrawing or donating groups (cyclopropanes **15** and **16** respectively) led to a reduction in reaction enantioselectivity. In contrast, bulky alkyl groups on the benzoate moiety increased the reaction *ee*; *p*-*t*Bu benzoyl cyclopropane **17** and 3,5-di-*t*Bu substituted cyclopropane **18** were produced in good yield and enantioselectivity. Cyclopropanes **9** - **18** were isolated by flash chromatography prior to HPLC analysis; the catalyst and any associated decomposition products were readily removed from the product mixture.

Figure 3. Cyclopropane Products Synthesized Using [Au((R_{mp})-6)(Cl)][a]

cis-**9**
86% (88% *de*, 57% *ee*)

cis-**10**
53% (84% *de*, 50% *ee*)

cis-**11**
25% (92% *de*, 46% *ee*)

cis-**12**
73% (62% *de*, 42% *ee*)

cis-**13**
90% (92% *de*, 9% *ee*)

cis-**14**
40% (92% *de*, 54% *ee*)

cis-**15**
45% (92% *de*, 45% *ee*)

cis-**16**
48% (88% *de*, 41% *ee*)

cis-**17**
79% (90% *de*, 74% *ee*)

cis-**18**
68% (90% *de*, 77% *ee*)

[a]All reactions carried out under the conditions shown in Table 1, Entry 8. Combined yields of cyclopropanes and *de* were determined by ^{1}H NMR analysis of the crude reaction product using $C_2Cl_4H_2$ as an internal standard. *ee* of the major *cis* diastereomer determined by HPLC analysis of purified samples.[57]

Modelling of the Au[I]-Mediated Cyclopropanation of Styrene

Detailed modelling of interlocked molecules is challenging given both their size and flexibility. Previously, the catalytic behaviour of an interlocked catenane organocatalyst was studied computationally by considering the catalytic fragment alone on the assumption that the rest of the structure did not play a direct role in the reaction.[58] In the case of [Au(**6**)(Cl)] this clearly would not be a reasonable assumption as the mechanical bond is the sole source of stereochemistry. Also, the implied difference in activation barrier, even for the most selective example reported above (**18**) is only ~4.5 kJmol[−1], a relatively small value for such a complex system where multiple conformations of the catalyst may be mechanistically relevant. These caveats notwithstanding, in order to gain some qualitative insight into how interactions between the reacting substrates and the rotaxane structure might influence the stereoselectivity of the reaction we conducted preliminary computational modelling of the reaction of propargylic ester **7** and styrene (**8**) mediated by [Au(R_{mp}-**6**)(Cl)].

In brief (for full details see ESI), we began by locating the lowest energy transition state (CAM-B3LYP/6-31G*/SDD(Au)) for the reaction of **7** with **8** mediated by [Au(PPh₃)(Cl)], building on previous work by Echavarren and co-workers.[59] In keeping with this previous report, the reaction of the carbene derived from **7** with **8** was found to be a two-step process. We thus assumed a similar pathway for the reaction mediated by [Au(**6**)(Cl)] (Figure 4A); coordination of Cu[I] and abstraction of the Cl ligand gives rise to proposed active catalyst [AuCu(**6**)]²⁺ which coordinates to alkyne **7** to give complex **I** that undergoes a rearrangement to produce key carbene intermediate **II**. Addition of styrene to **II** produces carbocation **III** *via* key transition state **TSI**, in the process setting the stereochemistry of C¹ of the cyclopropane product. Subsequent rapid ring closure gives rise to cyclopropane **9** and regenerates the catalyst.

Figure 4. Reaction Pathway and Modelled Transition State Structures
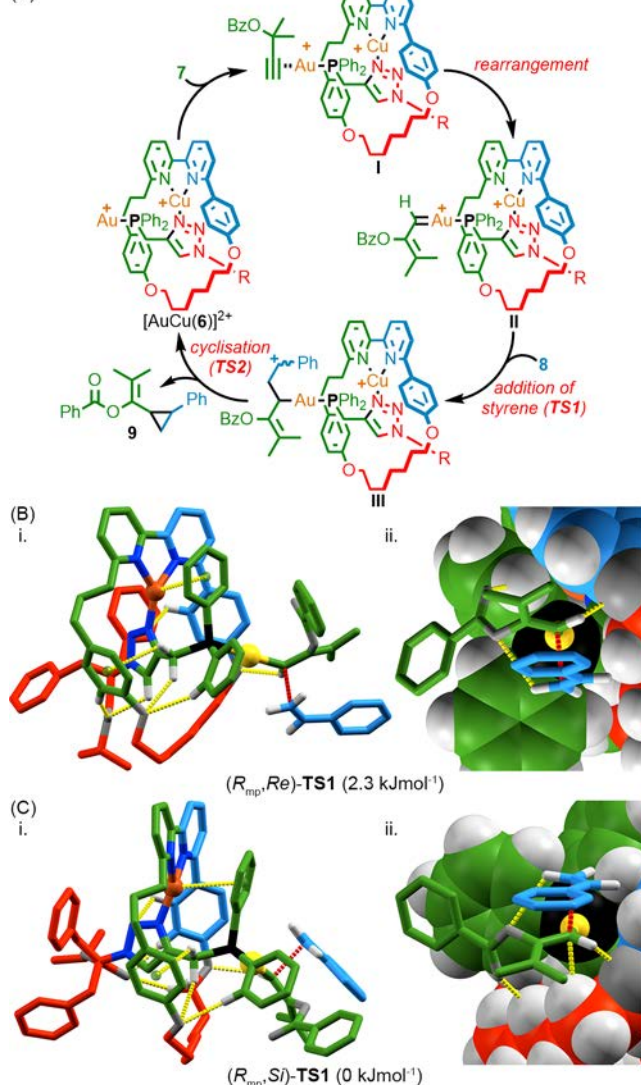
(A) Reaction pathway presumed for the reaction of [Au(**6**)(Cl)] based on molecular modelling (Gaussian '09, CAM-B3LYP, 6-31G*/SDD(Au)) of the reaction of **7** and **8** mediated by [Au(PPh₃)(Cl)]. R = C(Bn)₂CO₂ⁱPr.

(B) Modelled (CHCl₃, CAM-B3LYP, 6-31G/SDD) structure of **TS1** leading to (1*R*,2*S*)-**9** for the reaction of **7** with **8** mediated by [AuCu((*R*ₘₚ)-**6**)]²⁺ in (i) sticks representation and (ii) close up of the transition state fragment in mixed space-filling and sticks representation. Selected intercomponent interactions and the carbene-styrene interaction associated with the reaction coordinate are highlighted in yellow and red respectively.

(C) Modelled (CHCl₃, CAM-B3LYP, 6-31G/SDD) structure of **TS1** leading to (1*S*,2*R*)-**9** for the reaction of **7** with **8** mediated by [AuCu((*R*ₘₚ)-**6**)]²⁺ in (i) sticks representation and (ii) close up of the transition state fragment in mixed space-filling and sticks representation. Selected intercomponent interactions and the carbene-styrene interaction associated with the reaction coordinate are highlighted in yellow and red respectively.

In order to investigate the reaction mediated by rotaxane [Au(**6**)(Cl)], the transition state model found for the reaction mediated by [Au(PPh₃)(Cl)] was modified by attachment to the Cuᴵ-coordinated metallorotaxane.[60] A conformational search (Spartan '10, MMF)[61] with the transition state fragment frozen yielded low energy conformers for each diastereomeric complex which were optimised using DFT (Gaussian '09,[62] CAM-B3LYP, 6-31G/SDD(Cu,Au)), again with the transition state fragment frozen, to identify the lowest energy conformation. Transition state optimisation, first using an Oniom method (CAM-B3LYP:UFF, 6-31G/SDD(Au)), followed by a full DFT optimisation (CAM-B3LYP, 631G/SDD(Cu,Au)) first in the gas phase then in solvent (CHCl₃, polarizable continuum model) yielded transition state models (*R*ₘₚ,*Re*)-**TS1** and (*R*ₘₚ,*Si*)-**TS1** (Figures 4B and 4C respectively) that were determined to be first order saddle points with a single imaginary frequency.

Examining the models of (R_{mp},Re)-**TS1** and (R_{mp},Si)-**TS1** (Figures 4B and 4C respectively) reveals that, in spite of their size and large number of rotatable bonds, the modelled catalyst structure is actually relatively rigid due to steric crowding combined with the coordination of the Cu^I ion. A complex network of short intra- and inter-component contacts, including CH hydrogen bonds, CH-π interactions and cation-π interaction between the Cu^I ion and one of the Ph rings of the phosphine ligand are predicted to stabilise the system further and project the Au^I centre bearing the reactive carbene moiety towards the macrocycle, into the space around one of the phenoxy ether moieties. It is perhaps noteworthy that the optimised structures are similar to the solid-state structures of rotaxanes **4** determined by x-ray diffraction in which the phosphine substituent (O) is also projected towards the same aryl ether moiety. Crowding around the Au^I carbene moiety due to the mechanical bond is clearly seen in the space-filling models of (R_{mp},Re)-**TS1** and (R_{mp},Si)-**TS1** (Figure 4Bii and Cii respectively); the macrocycle provides a sterically crowded environment that shields one face of the carbene unit and restricts the rotation of the substrate around the Au-P axis. The substrates are stabilised in the rotaxane environment through a number of non-covalent interactions, in particular a C(carbene)H-O interaction in both structures and a CH-C(carbene) interaction in the case of (R_{mp},Si)-**TS1**. Thus, the modelling suggests that mechanically bonded structure provides a well-expressed chiral environment for the catalysis to take place within, which is consistent with the reasonable enantioselectivities achieved experimentally.

Finally, comparison of the calculated relative energies of (R_{mp},Re)-**TS1** and (R_{mp},Si)-**TS1** revealed remarkable agreement, given the size of the system, between experiment and theory; (R_{mp},Si)-**TS1** was found to be favoured by ~2.3 kJmol^{-1}, corresponding to a stereoselectivity of 74 : 26 in favour of the major observed product (1S,2R)-**9**. However, caution should be taken when interpreting this level of agreement; modelling in the the gas phase (6-31G/SDD) predicted the opposite stereoselectivity ((R_{mp},Re)-**TS1** favoured by ~1.7 kJmol^{-1}). Conversely re-optimisation of **TS1** with the larger 6-31G* basis set in the gas phase or in CHCl$_3$ (single point calculation)[63] resulted in a predicted selectivity for the correct diastereomer that exceeds what is observed experimentally, demonstrating the uncertainty in the absolute values generated in such complex systems. Furthermore, although extending the modelling to the reactions leading to cyclopropanes **15** and **16** revealed reasonable agreement with experiment, the same calculations for the reaction leading to cyclopropanes **13** predicted a high selectivity, in contrast to the low selectivity observed experimentally (see ESI for details).

Thus, the molecular models of (R_{mp},Re)-**TS1** and (R_{mp},Si)-**TS1** should be considered qualitative, providing some insight into the potential interactions and a pictorial representation of the chiral environment created by the mechanical bond around the reacting Au^I carbene. A more detailed study, combined with many more comparisons between experiment and theory, would be required to determine the details of the key intermolecular interactions that lead to the observed stereoselectivity.

CONCLUSIONS

Although the first enantiopure mechanically planar chiral rotaxane was reported over two decades ago[13] this is, to our knowledge, the first time that this stereogenic unit has been applied in catalysis. The results presented clearly demonstrate that the mechanically planar chiral stereogenic unit can direct enantioselective catalysis. The results are particularly pleasing given that rotaxane **6** was not explicitly designed or optimised for the reaction presented and yet achieves stereoselectivities with benzoate esters of 42 - 77% *ee*, comparable to a similar reaction mediated by optimised covalent catalyst (*R*)-DTBM-SEGPHOS®(AuCl)$_2$ (68% *ee*). By extension, our results suggest that other mechanical stereogenic units[6] such as the axial and topological chiral units in catenanes have unexplored potential in catalytic applications.

However, the stereoselectivities observed in this cyclopropanation reaction are lower than those reported when pivloate esters, which are not tolerated by [Au(**6**)(Cl)], were employed with the best covalent catalysts (76 to 94% *ee*),[41] clearly demonstrating that challenges remain to be overcome for mechanically chiral rotaxanes to become useful tools in organic synthesis. It should also be noted that preliminary attempts to apply [Au(**6**)(Cl)] to other Au^I-mediated reactions were unsuccessful (see ESI), suggesting that our success in this one reaction is serendipitous, rather than an indication that the mechanically planar chiral stereogenic unit is somehow a "magic bullet" for enantioselective gold catalysis. Indeed, this

is consistent with results with covalent catalysts (e.g. (*R*)-DTBM-SEGPHOS®(AuCl)$_2$ - see ESI) that have been optimised for one Au^I-mediated reaction but often perform poorly in others.[64] Furthermore, despite recent progress in the area,[38,39,40] the synthesis of mechanically interlocked molecules is still challenging, in the example presented specifically due to the low stereoselectivity observed in the mechanical bond forming step and the epimerisation of the stereodirecting unit derived from the α-chiral azide that complicates the purification. This synthetic challenge clearly complicates the optimisation of catalyst frameworks to deliver enhanced enantioselectivity. However, recent progress in the development of new methodologies to access enantiopure mechanically chiral molecules suggests that this synthetic challenge can and is being addressed, and pleasingly, based on the preliminary molecular modelling presented, it seems that modern computational chemistry may well be able to aid the design process.

Thus, in the future, we see a place for mechanical chirality in catalysis, particularly where it is otherwise challenging to project chiral information into the reaction space, as in the Au^I-mediated reaction presented here; the crowded, three-dimensional [65] nature of the mechanical bond appears to be well suited to generating a chiral pocket for chemical reactions to take place within, similar in some ways to enzymatic active sites with their combination of steric hindrance and weak attractive interactions with the substrate. Furthermore, combining chiral mechanical stereogenic units with the well-developed chemistry of interlocked molecular shuttles[2, 66] should allow the influence of the stereogenic mechanical bond to be modulated[67] in a stimuli responsive manner in order to develop switchable chiral catalysts, for instance to produce both hands of a given chiral product in high enantioselectivity.[68] Indeed, during the preparation of this manuscript this principle was demonstrated in the context of co-conformational covalent point chirality.[69] The same principles may also hold in the development of enantioselective sensors for chiral molecules. What is clear, based on these results, is that the chemical applications[70] of mechanically chiral interlocked molecules deserve further investigation.

SUPPLEMENTAL INFORMATION

Supplemental Information includes experimental procedures and characterization data for rotaxanes **4**, **5** and [Au(**6**)(Cl)], cyclopropanes **9**-**18** and their precursors, as well as full details of the computational modelling carried out. Crystallographic data and coordinates of model structures, both in CIF format, are provided as separate files.

AUTHOR CONTRIBUTIONS

S.M.G. conceived the project and secured project funding. A.W.H contributed to the design of experiments and methodology, and executed all experimental procedures. S.M.G. carried out the computational modelling. S.M.G. wrote the manuscript with input from A.W.H. Both authors contributed to the reviewing and editing of the manuscript.

DECLARATION OF INTERESTS

The authors declare no competing interests.

REFERENCES AND NOTES

1. Bruns, C. J. & Stoddart, J. F. (Wiley, 2016). *The Nature of the Mechanical Bond: From Molecules to Machines.*
2. Erbas-Cakmak, S., Leigh, D. A., McTernan, C. T. & Nussbaumer, A. L. (2015). Artificial Molecular Machines. *Chem. Rev.* **115**, 10081–10206.
3. Stoddart, J. F. (2017). Mechanically Interlocked Molecules (MIMs)—Molecular Shuttles, Switches, and Machines (Nobel Lecture). *Angew. Chem. Int. Ed.* **56**, 11094–11125.
4. Sauvage, J. P. (2017). From Chemical Topology to Molecular Machines (Nobel Lecture). *Angew. Chem. Int. Ed.* **56**, 11080–11093.
5. Feringa was co-awarded the 2016 Nobel Prize for Chemistry in recognition of his work on non-interlocked molecular machines: Feringa, B. L. (2017). The Art of Building Small: From Molecular Switches to Motors (Nobel Lecture). *Angew. Chem. Int. Ed.* **56**, 11060–11078.
6. Reviews: Jamieson, E. M. G., Modicom, F. & Goldup, S. M. (2018). Chirality in rotaxanes and catenanes. *Chem. Soc. Rev.* **47**, 5266–5311. Pairault, N. & Niemeyer, J. (2018). Chiral Mechanically Interlocked Molecules – Applications of Rotaxanes, Catenanes and Molecular Knots in Stereoselective Chemosensing and Catalysis. *Synlett* **29**, 689–698. Evans, N. H. (2018). Chiral Catenanes and Rotaxanes: Fundamentals and Emerging Applications. *Chem. - A Eur. J.* **24**, 3101–3112.
7. Frisch, H. L. & Wasserman, E. (1961). Chemical Topology. *J. Am. Chem. Soc.* **83**, 3789–3795
8. Schill, G. (Academic Press, 1971). *Catenanes, Rotaxanes and Knots.*
9. Dálaigh, C. Ó., Hynes, S. J., Maher, D. J. & Connon, S. J. (2005). Kinetic resolution of sec-alcohols using a new class of readily assembled (S)-proline-derived 4-(pyrrolidino)-pyridine analogues. *Org. Biomol. Chem.* **3**, 981–984.
10. Spivey, A. C., Zhu, F., Mitchell, M. B., Davey, S. G. & Jarvest, R. L. (2003). Concise Synthesis, Preparative Resolution, Absolute Configuration Determination, and Applications of an Atropisomeric Biaryl Catalyst for Asymmetric Acylation. *J. Org. Chem.* **68**, 7379–7385
11. Ruble, J. C., Latham, H. A. & Fu, G. C. (1997). Effective kinetic resolution of secondary alcohols with a planar-chiral analogue of 4-(dimethylamino)pyridine. Use of the Fe(C5H5) group in asymmetric catalysis. *J. Am. Chem. Soc.* **119**, 1492–1493
12. Crittall, M. R., Rzepa, H. S. & Carbery, D. R. (2011). Design, synthesis, and evaluation of a helicenoidal DMAP lewis base catalyst. *Org. Lett.* **13**, 1250–1253
13. Yamamoto, C., Okamoto, Y., Schmidt, T., Jäger, R. & Vögtle, F. (1997). Enantiomeric Resolution of Cycloenantiomeric Rotaxane, Topologically Chiral Catenane, and Pretzel-Shaped Molecules: Observation of Pronounced Circular Dichroism. *J. Am. Chem. Soc.* **119**, 10547–10548.
14. Kaida, Y., Okamoto, Y., Chambron, J.-C., Mitchell, D. K. & Sauvage, J.-P. (1993). The separation of optically active copper (I) catenates. *Tetrahedron Lett.* **34**, 1019–1022.
15. Hirose, K., Ukimi, M., Ueda, S., Onoda, C., Kano, R., Tsuda, K., Hinohara, Y. & Tobe, Y. (2018). The Asymmetry is Derived from Mechanical Interlocking of Achiral Axle and Achiral Ring Components – Syntheses and Properties of Optically Pure [2]Rotaxanes–. *Symmetry (Basel).* **10**, 20.
16. Ishiwari, F., Nakazono, K., Koyama, Y. & Takata, T. (2017). Induction of Single-Handed Helicity of Polyacetylenes Using Mechanically Chiral Rotaxanes as Chiral Sources. *Angew. Chem. Int. Ed.* **56**, 14858–14862.
17. Mochizuki, Y., Ikeyatsu, K., Mutoh, Y., Hosoya, S. & Saito, S. (2017). Synthesis of Mechanically Planar Chiral rac- [2]Rotaxanes by Partitioning of an Achiral [2]Rotaxane: Stereoinversion Induced by Shuttling. *Org. Lett.* **19**, 4347–4350.
18. Corra, S., de Vet, C., Groppi, J., La Rosa, M., Silvi, S., Baroncini, M. & Credi, A. (2019). Chemical On/Off Switching of Mechanically Planar Chirality and Chiral Anion Recognition in a [2]Rotaxane Molecular Shuttle. *J. Am. Chem. Soc.* **141**, 9129–9133.
19. Cakmak, Y., Erbas-Cakmak, S. & Leigh, D. A. (2016). Asymmetric Catalysis with a Mechanically Point-Chiral Rotaxane. *J. Am. Chem. Soc.* **138**, 1749–1751.
20. The same authors have developed molecular ratchets and motors based on this stereogenic element. See: Alvarez-Pérez, M., Goldup, S. M., Leigh, D. A. & Slawin, A. M. Z. (2008). A Chemically-Driven Molecular Information Ratchet. *J. Am. Chem. Soc.* **130**, 1836–1838; Carlone, A., Goldup, S. M., Lebrasseur, N., Leigh, D. A. & Wilson, A. (2012). A Three-Compartment Chemically-Driven Molecular Information Ratchet. *J. Am. Chem. Soc.* **134**, 8321–8323.
21. Goldup, S. M. (2016). A chiral catalyst with a ring to it. *Nat. Chem.* **8**, 404–406.
22. Eliel, E., Wilen, S. & Mander, L. (John Wiley and Sons, Inc., 1994). *Stereochemistry of Organic Compounds.*
23. Dálaigh, C. Ó., Hynes, S. J., Maher, D. J. & Connon, S. J. (2005). Kinetic resolution of sec-alcohols using a new class of readily assembled (S)-proline-derived 4-(pyrrolidino)-pyridine analogues. *Org. Biomol. Chem.* **3**, 981–984
24. Spivey, A. C., Zhu, F., Mitchell, M. B., Davey, S. G. & Jarvest, R. L. (2003). Concise synthesis, preparative resolution, absolute configuration determination, and applications of an atropisomeric biaryl catalyst for asymmetric acylation. *J. Org. Chem.* **68**, 7379–7385
25. Ruble, J. C., Latham, H. A. & Fu, G. C. (1997). Effective kinetic resolution of secondary alcohols with a planar-chiral analogue of 4-(dimethylamino)pyridine. Use of the Fe(C5Ph5) group in asymmetric catalysis. *J. Am. Chem. Soc.* **119**, 1492–1493
26. Crittall, M. R., Rzepa, H. S. & Carbery, D. R. (2011). Design, synthesis, and evaluation of a helicenoidal DMAP lewis base catalyst. *Org. Lett.* **13**, 1250–1253.
27. By chirotopic elements, we mean stereogenic units around that are locally chiral (see: Mislow, K. & Siegel, J. (1984). Stereoisomerism and local chirality. *J. Am. Chem. Soc.* **106**, 3319–3328). Similarly, when we describe a molecule as "mechanically planar chiral" (or similar) this is shorthand for a molecule that is chiral as a consequence of containing the mechanical planar chiral stereogenic unit.
28. Noyori, R. (2002). Asymmetric catalysis: Science and opportunities (nobel lecture). *Angew. Chem. Int. Ed.* **41**, 2008–2022.
29. Knowles, W. S. (2002). Asymmetric Hydrogenations (Nobel Lecture). *Angew. Chem. Int. Ed.* **41**, 1998–2007.
30. Sharpless, K. B. (2002). Searching for New Reactivity (Nobel Lecture). *Angew. Chem. Int. Ed.* **41**, 2024–2032.
31. Phipps, R. J., Hamilton, G. L. & Toste, F. D. (2012). The progression of chiral anions from concepts to applications in asymmetric catalysis. *Nat. Chem.* **4**, 603–614.
32. Hong, Y., Jarrige, L., Harms, K. & Meggers, E. (2019). Chiral-at-Iron Catalyst: Expanding the Chemical Space for Asymmetric Earth-Abundant Metal Catalysis. *J. Am. Chem. Soc.* **141**, 4569–4572.

33. Yashima, E., Maeda, K., Iida, H., Furusho, Y. & Nagai, K. (2009). Helical Polymers: Synthesis, Structures, and Functions. *Chem. Rev.* **109**, 6102–6211.

34. Boersma, A. J., Megens, R. P., Feringa, B. L. & Roelfes, G. (2010). DNA-based asymmetric catalysis. *Chem. Soc. Rev.* **39**, 2083–2092; Silverman, S. K. (2010). DNA as a Versatile Chemical Component for Catalysis, Encoding, and Stereocontrol. *Angew. Chem. Int. Ed.* **49**, 7180–7201.

35. Nagata, Y., Takeda, R. & Suginome, M. (2019). Asymmetric Catalysis in Chiral Solvents: Chirality Transfer with Amplification of Homochirality through a Helical Macromolecular Scaffold. *ACS Cent. Sci.* **5**, 1235–1240.

36. Tan, C., Chu, D., Tang, X., Liu, Y., Xuan, W. & Cui, Y. (2019). Supramolecular Coordination Cages for Asymmetric Catalysis. *Chem. - A Eur. J.* **25**, 662–672.

37. Zhang, P., Tugny, C., Meijide Suárez, J., Guitet, M., Derat, E., Vanthuyne, N., Zhang, Y., Bistri, O., Mouriès-Mansuy, V., Ménand, M., Roland, S., Fensterbank, L. & Sollogoub, M. (2017). Artificial Chiral Metallo-pockets Including a Single Metal Serving as Structural Probe and Catalytic Center. *Chem* **3**, 174–191.

38. Bordoli, R. J. & Goldup, S. M. (2014). An Efficient Approach to Mechanically Planar Chiral Rotaxanes. *J. Am. Chem. Soc.* **136**, 4817–4820.

39. Jinks, M. A., de Juan, A., Denis, M., Fletcher, C. J., Galli, M., Jamieson, E. M. G., Modicom, F., Zhang, Z. & Goldup, S. M. (2018). Stereoselective Synthesis of Mechanically Planar Chiral Rotaxanes. *Angew. Chem. Int. Ed.* **57**, 14806–14810.

40. Denis, M., Lewis, J. E. M., Modicom, F. & Goldup, S. M. (2019). An Auxiliary Approach for the Stereoselective Synthesis of Topologically Chiral Catenanes. *Chem* **5**, 1512–1520.

41. Johansson, M. J., Gorin, D. J., Staben, S. T. & Toste, F. D. (2005). Gold(I)-Catalyzed Stereoselective Olefin Cyclopropanation. *J. Am. Chem. Soc.* **127**, 18002–18003.

42. Wang, Y. M., Lackner, A. D. & Toste, F. D. (2014). Development of catalysts and ligands for enantioselective gold catalysis. *Acc. Chem. Res.* **47**, 889–901.

43. Wang, Y. M., Lackner, A. D. & Toste, F. D. (2014). Development of catalysts and ligands for enantioselective gold catalysis. *Acc. Chem. Res.* **47**, 889–901. Zi, W. & Dean Toste, F. (2016). Recent advances in enantioselective gold catalysis. *Chem. Soc. Rev.* **45**, 4567–4589.

44. Wang, Z., Nicolini, C., Hervieu, C., Wong, Y. F., Zanoni, G. & Zhang, L. (2017). Remote Cooperative Group Strategy Enables Ligands for Accelerative Asymmetric Gold Catalysis. *J. Am. Chem. Soc.* **139**, 16064–16067. Wang, Y., Zhang, P., Di, X., Dai, Q., Zhang, Z. M. & Zhang, J. (2017). Gold-Catalyzed Asymmetric Intramolecular Cyclization of N-Allenamides for the Synthesis of Chiral Tetrahydrocarbolines. *Angew. Chem. Int. Ed.* **56**, 15905–15909.

45. For a recent example of an elegant design strategy to control the enantioselective folding of an enyne substrate on a π-surface see: Zuccarello, G., Mayans, J. G., Escofet, I., Scharnagel, D., Kirillova, M. S., Pérez-Jimeno, A. H., Calleja, P., Boothe, J. R. & Echavarren, A. M. (2019). Enantioselective Folding of Enynes by Gold(I) Catalysts with a Remote C 2 -Chiral Element. *J. Am. Chem. Soc.* **141**, 11858–11863.

46. Galli, M., Lewis, J. E. M. & Goldup, S. M. (2015). A Stimuli-Responsive Rotaxane-Gold Catalyst: Regulation of Activity and Diastereoselectivity. *Angew. Chem. Int. Ed.* **54**, 13545–13549.

47. Lahlali, H., Jobe, K., Watkinson, M. & Goldup, S. M. (2011). Macrocycle Size Matters: "Small" Functionalized Rotaxanes in Excellent Yield Using the CuAAC Active Template Approach. *Angew. Chem. Int. Ed.* **50**, 4151–4155.

48. Denis, M. & Goldup, S. M. (2017). The active template approach to interlocked molecules. *Nat. Rev. Chem.* **1**, 0061.

49. Aucagne, V., Hänni, K. D., Leigh, D. A., Lusby, P. J. & Walker, D. B. (2006). Catalytic "Click" Rotaxanes: A Substoichiometric Metal-Template Pathway to Mechanically Interlocked Architectures. *J. Am. Chem. Soc.* **128**, 2186–2187. Aucagne, V., Berna, J., Crowley, J. D., Goldup, S. M., Hänni, K. D., Leigh, D. A., Lusby, P. J., Ronaldson, V. E., Slawin, A. M. Z., Viterisi, A. & Walker, D. B. (2007). Catalytic 'active-metal' template synthesis of [2]rotaxanes, [3]rotaxanes, and molecular shuttles, and some observations on the mechanism of the cu(i)-catalyzed azide-alkyne 1,3-cycloaddition. *J. Am. Chem. Soc.* **129**, 11950–11963.

50. Lewis, J. E. M., Bordoli, R. J., Denis, M., Fletcher, C. J., Galli, M., Neal, E. A., Rochette, E. M. & Goldup, S. M. (2016). High yielding synthesis of 2,2′ -bipyridine macrocycles, versatile intermediates in the synthesis of rotaxanes. *Chem. Sci.* **7**, 3154–3161.

51. Care must be taken in the separation of diastereomers **4** as the covalent stereogenic centre is prone to epimerisation. See ESI for full details.

52. Although the SC-XRD-derived solid state structure of (*S*,*R*mp)-**4** is of high quality, the single-crystal of (*S*,*S*mp)-**4** appears to be contaminated with an oxidised derivative of the rotaxane. The structure of (*S*,*R*mp)-**4** alone is sufficient to assign the relative and, using the known stereochemistry of the azide derived component, the absolute stereochemistry of both diastereomers. However, the SC-XRD-derived structure of (*S*,*S*mp)-**4** is of good quality once the impurity is taken into account and, importantly, the relative stereochemistry observed is, as expected, epimeric with that determined for (*S*,*R*mp)-**4**. For full details see ESI.

53. SC-XRD allows the relative stereochemistry of the mechanical bond and covalent stereogenic unit to be determined unambiguously for the diastereomeric rotaxanes. This information, combined with the known configuration of the azide-derived stereogenic unit, allows the absolute stereochemistry of rotaxanes **4**, and their derivatives, to be determined.

54. Miki, K., Ohe, K. & Uemura, S. (2003). A new ruthenium-catalyzed cyclopropanation of alkenes using propargylic acetates as a precursor of vinylcarbenoids. *Tetrahedron Lett.* **44**, 2019–2022.

55. Teller, H., Flügge, S., Goddard, R. & Fürstner, A. (2010). Enantioselective gold catalysis: Opportunities provided by monodentate phosphoramidite ligands with an acyclic TADDOL backbone. *Angew. Chem. Int. Ed.* **49**, 1949–1953

56. Gross, E., Liu, J. H., Alayoglu, S., Marcus, M. A., Fakra, S. C., Toste, F. D. & Somorjai, G. A. (2013). Asymmetric catalysis at the mesoscale: Gold nanoclusters embedded in chiral self-assembled monolayer as heterogeneous catalyst for asymmetric reactions. *J. Am. Chem. Soc.* **135**, 3881–3886.

57. The absolute stereochemistry of (1*S*,2*R*)-**9** was assigned by comparison with the product of the reaction mediated by (*R*)-DTBM-SEGPHOS®(AuCl)₂, the stereochemical outcome of which is known.[41] The absolute configurations of *cis*-**15**, *cis*-**16** and *cis*-**18** were determined to be (1*S*,2*R*) by convergence to the same reduction product as that produced by *cis*-**9** (see ESI for details). The absolute stereochemistry of all other cyclopropane products was not determined. The (1*S*,2*R*) products are shown but this assignment is arbitrary.

58 Mitra, R., Zhu, H., Grimme, S. & Niemeyer, J. (2017). Functional Mechanically Interlocked Molecules: Asymmetric Organocatalysis with a Catenated Bifunctional Brønsted Acid. *Angew. Chem. Int. Ed.* **56**, 11456–11459.

59 Pérez-Galán, P., Herrero-Gómez, E., Hog, D. T., Martin, N. J. A., Maseras, F. & Echavarren, A. M. (2011). Mechanism of the gold-catalyzed cyclopropanation of alkenes with 1,6-enynes. *Chem. Sci.* **2**, 141–149

60 It is an open question whether an interlocked molecule in which the components are bridged in this manner are true rotaxanes or if the metal-ligand interactions constitute a covalent link, rendering them entangled but not mechanically bonded, strictly speaking. Sauvage employed the term "catenate" to denote such complexes in the context of catenanes,[14] but the equivalent noun "rotaxanate" is more commonly used as a verb meaning "to make a rotaxane" (for examples where rotaxanate is used as a noun see: Furusho, Y., Matsuyama, T., Takata, T., Moriuchi, T. & Hirao, T. (2004). Synthesis of novel interlocked systems utilizing a palladium complex with 2,6-pyridinedicarboxamide-based tridentate macrocyclic ligand. *Tetrahedron Lett.* **45**, 9593–9597; Mateo-Alonso, A. (2010). Mechanically interlocked molecular architectures functionalised with fullerenes. *Chem. Commun.* **46**, 9089–9099; Miyagawa, N., Watanabe, M., Matsuyama, T., Koyama, Y., Moriuchi, T., Hirao, T., Furusho, Y. & Takata, T. (2010). Successive catalytic reactions specific to Pd-based rotaxane complexes as a result of wheel translation along the axle. *Chem. Commun.* **46**, 1920–1922). Here we use the term "metallorotaxane", which has seen some use to denote the mechanically chelated complex, rather than "rotaxanate", to avoid confusion.[1]

61 Spartan '10, Wavfunction Inc.

62 Frisch, M. J., Trucks, G. W., Schlegel, H. B., Scuseria, G. E., Robb, M. A., Cheeseman, J. R., Scalmani, G., Barone, V., Mennucci, B., Petersson, G. A., Nakatsuji, H., Caricato, M., Li, X., Hratchian, H. P., Izmaylov, A. F., Bloino, J., Zheng, G., Sonnenberg, J. L., Hada, M., Ehara, M., Toyota, K., Fukuda, R., Hasegawa, J., Ishida, M., Nakajima, T., Honda, Y., Kitao, O., Nakai, H., Vreven, T., Montgomery Jr., J. A., Peralta, J. E., Ogliaro, F., Bearpark, M., Heyd, J. J., Brothers, E., Kudin, K. N., Staroverov, V. N., Keith, T., Kobayashi, R., Normand, J., Raghavachari, K., Rendell, A., Burant, J. C., Iyengar, S. S., Tomasi, J., Cossi, M., Rega, N., Millam, J. M., Klene, M., Knox, J. E., Cross, J. B., Bakken, V., Adamo, C., Jaramillo, J., Gomperts, R., Stratmann, R. E., Yazyev, O., Austin, A. J., Cammi, R., Pomelli, C., Ochterski, J. W., Martin, R. L., Morokuma, K., Zakrzewski, V. G., Voth, G. A., Salvador, P., Dannenberg, J. J., Dapprich, S., Daniels, A. D., Farkas, O., Foresman, J. B., Ortiz, J. V., Cioslowski, J. & Fox, D. J. (2013). Gaussian '09.

63 Single point energy calculation based on the gas phase 6-31G* structure; transition state optimisation using the 6-31G* basis set in solvent proved prohibitively computationally expensive.

64 For a recent detailed study in which a very large number of previously successful ligands for Au[I] enantioselective catalysis were screened, often with poor results, in a new reaction see: Zuccarello, G., Mayans, J. G., Escofet, I., Scharnagel, D., Kirillova, M. S., Pérez-Jimeno, A. H., Calleja, P., Boothe, J. R. & Echavarren, A. M. (2019). Enantioselective Folding of Enynes by Gold(I) Catalysts with a Remote C2-Chiral Element. *J. Am. Chem. Soc.* **141**, 11858–11863

65 For examples in which covalent chiral information is transferred through the mechanical bond see: Tachibana, Y., Kihara, N. & Takata, T. (2004). Asymmetric Benzoin Condensation Catalyzed by Chiral Rotaxanes Tethering a Thiazolium Salt Moiety via the Cooperation of the Component: Can Rotaxane Be an Effective Reaction Field? *J. Am. Chem. Soc.* **126**, 3438–3439; Xu, K., Nakazono, K. & Takata, T. (2016). Design of Rotaxane Catalyst for *O*-Acylative Asymmetric Desymmetrization of *meso*-1,2-Diol Utilizing the Cooperative Effect of the Components. *Chem. Lett.* **45**, 1274–1276.

66 For examples of switchable catalysts based on rotaxane molecular shuttles see: Blanco, V., Carlone, A., Hänni, K. D., Leigh, D. A. & Lewandowski, B. (2012). A rotaxane-based switchable organocatalyst. *Angew. Chem. Int. Ed.* **51**, 5166–5169; Blanco, V., Leigh, D. A., Lewandowska, U., Lewandowski, B. & Marcos, V. (2014). Exploring the Activation Modes of a Rotaxane-Based Switchable Organocatalyst. *J. Am. Chem. Soc.* **136**, 15775–15780; Eichstaedt, K., Jaramillo-Garcia, J., Leigh, D. A., Marcos, V., Pisano, S. & Singleton, T. A. (2017). Switching between Anion-Binding Catalysis and Aminocatalysis with a Rotaxane Dual-Function Catalyst. *J. Am. Chem. Soc.* **139**, 9376–9381; Blanco, V., Leigh, D. A., Marcos, V., Morales-Serna, J. A. & Nussbaumer, A. L. (2014). A switchable [2]rotaxane asymmetric organocatalyst that utilizes an acyclic chiral secondary amine. *J. Am. Chem. Soc.* **136**, 4905–4908.

67 Suzuki, S., Ishiwari, F., Nakazono, K. & Takata, T. (2012). Reversible helix–random coil transition of poly(m-phenylenediethynylene) by a rotaxane switch. *Chem. Commun.* **48**, 6478–6480.

68 For examples of non-interlocked molecular machines that control the stereoselective synthesis of molecules see: Wang, J. & Feringa, B. L. (2011). Dynamic Control of Chiral Space in a Catalytic Asymmetric Reaction Using a Molecular Motor. *Science (80-.).* **331**, 1429–1432; Kassem, S., Lee, A. T. L., Leigh, D. A., Marcos, V., Palmer, L. I. & Pisano, S. (2017). Stereodivergent synthesis with a programmable molecular machine. *Nature* **549**, 374–378.

69 Dommaschk, M., Echavarren, J., Leigh, D., Marcos, V. & Singleton, T. A. (2019). Dynamic Control of Chiral Space Through Local Symmetry Breaking in a Rotaxane Organocatalyst. *Angew. Chem. Int. Ed.* doi:10.1002/anie.201908330.

70 Sluysmans, D. & Stoddart, J. F. (2019). The Burgeoning of Mechanically Interlocked Molecules in Chemistry. *Trends Chem.* **1**, 185–197; Heard, A. W. & Goldup, S. M. (2020). Simplicity in the Design, Operation and Applications of Mechanically Interlocked Molecular Machines. *ACS Central Science* DOI: 10.1021/acscentsci.9b01185.